# Dynamics of Regional Lung Inflammation: New Questions and Answers Using PET

J. Batista Borges, G. Hedenstierna, and F. Suarez-Sipmann

## Introduction

> When the image is new, the world is new (Gaston Bachelard).
>
> The work of the eyes is done. Go now and do the heart-work on the images imprisoned within you (Rainer Maria Rilke).

The meaning of the term 'inflammation' has undergone considerable evolution. It was originally defined around the year 25 A.D. by Aulus Cornelius Celsus [1] and described the body's acute reaction following a traumatic event, such as a microscopic tear of a ligament or muscle. His original wording: "*Notae vero inflammationis sunt quatour: rubor et tumor cum calore et dolore*" (true signs of inflammation are four: redness and swelling with heat and pain) still holds. Disturbance of function (*functio laesa*) is the legendary fifth cardinal sign of inflammation and was added by Galen in the second century A.D. [2]. Recent articles [3] highlight the complicated role that inflammation plays in chronic illnesses, including metabolic, cardiovascular and neurodegenerative diseases. In addition to these difficult-to-treat diseases, more research and research tools are needed to illuminate therapeutic

J. Batista Borges
Hedenstierna laboratory, Department of Surgical Sciences, Section of Anesthesiology & Critical Care, Uppsala University, Uppsala, Sweden
Pulmonary Divison, Heart Institute (Incor) Hospital das Clínicas da Faculdade de Medicina da Universidade de São Paulo, São Paulo, Brazil

G. Hedenstierna
Hedenstierna laboratory, Department of Medical Sciences, Clinical Physiology, Uppsala University, Uppsala, Sweden

F. Suarez-Sipmann ✉
Hedenstierna laboratory, Department of Surgical Sciences, Section of Anesthesiology & Critical Care, Uppsala University, Uppsala, Sweden
CIBERES, Madrid, Spain
e-mail: fsuarez.sipmann@surgsci.uu.se

J.-L. Vincent (Ed.), *Annual Update in Intensive Care and Emergency Medicine 2014*,
DOI 10.1007/978-3-319-03746-2_15, 

strategies in another difficulty-to-treat inflammatory malady, the acute respiratory distress syndrome (ARDS).

In more than 40 years of extensive research on ARDS, little advance has been made in terms of outcome improvement [4] and much debate remains over pivotal concepts regarding the pathophysiology and almost every aspect of its treatment [5]. ARDS is a frequent and important cause of morbidity and mortality in critically ill patients [4, 6]. Some 74,500 persons die of acute lung injury (ALI) in the United States each year, a figure that is comparable to the number of adult deaths attributed to breast cancer or human immunodeficiency virus (HIV) disease in 1999 [6]. More importantly, ARDS occurs with a higher incidence than previously reported, currently estimated to be about 190,600 cases per year in the United States with a mortality rate of 38.5 %, and therefore has a substantial impact on public health [6].

## The Inflammatory Component of ARDS and Ventilator-induced Lung Injury

Dysregulated inflammation, inappropriate accumulation and activity of leukocytes and platelets, uncontrolled activation of coagulation pathways, and altered permeability of alveolar endothelial and epithelial barriers are central pathophysiologic concepts in ARDS [7–9]. Activation of the innate immune response by binding of microbial products or cell injury-associated endogenous molecules (danger-associated molecular patterns [DAMPs]) to pattern recognition receptors, such as the Toll-like receptors (TLRs) on the lung epithelium and alveolar macrophages, is now recognized as a potent driving force for acute lung inflammation. Newly reported innate immune effector mechanisms, such as formation of neutrophil extracellular traps – lattices of chromatin and antimicrobial factors that capture pathogens but can also cause endothelial injury – and histone release by neutrophils may contribute to alveolar injury. Signaling between inflammatory and hemostatic effector cells, such as platelet-neutrophil interaction, is also important. The delicate balance between protective and injurious innate and adaptive immune responses and hemostatic pathways may determine whether alveolar injury continues or is repaired and resolved.

Mechanical ventilation strategies designed to protect from the so-called ventilator-induced lung injury (VILI) reduce accumulation of pulmonary edema by preserving barrier properties of the alveolar endothelium and alveolar epithelium. Reductions in markers of lung epithelial injury have also been observed in clinical studies. These mechanical ventilation approaches aimed to attenuate VILI downregulate mechanosensitive pro-inflammatory pathways, resulting in reduced neutrophil accumulation in the alveoli and lower plasma levels of interleukin (IL)-6, IL-8, and soluble tumor necrosis factor (TNF) receptor 1.

VILI can induce or aggravate ARDS [10]. Mechanical cell deformation can be converted to biochemical changes, including production of pro-inflammatory cytokines. The proposed mechanism of VILI involves direct tissue damage due

to mechanical stretch and activation of specific intracellular pathways involved in 'mechanotransduction' [11]. Of note, the development of hyaline membranes and increased permeability require the presence of polymorphonuclear leukocytes (PMN), suggesting that in addition to mechanical damage, inflammation is also necessary for mechanical ventilation to induce injury.

Much controversy remains about the precise contribution, kinetics, and primary role of each one of the putative VILI mechanisms and how best to design a full-bodied mechanical ventilation strategy capable of minimizing the majority of them [12]. A pressing unanswered question remains over the relative role of lung cyclic stretch, in even moderate degrees, vs. low-volume injury. Low-volume injury promotes local concentration of stresses in the vicinity of collapsed regions in heterogeneously aerated lungs together with cyclical recruitment of airways and alveoli. This mechanism tends to predominate in more dependent regions of the lungs and to occur in previously damaged lungs prone to collapse [13, 14]. Tremblay et al. showed increased production of inflammatory cytokines in lungs ventilated without positive end-expiratory pressure (PEEP) [15]. Conversely, stretch tends to occur in non-dependent regions and results from increased regional lung volume. Overstretching of alveolar walls causes endothelial and epithelial breaks and interstitial edema. Detachment of endothelial cells from the basement membrane and death of epithelial cells with denuding of the epithelial basement membrane become obvious after 20 min of mechanical ventilation with very high tidal volumes ($V_T$) [16]. The excessive deformation of epithelial and endothelial cells, as well as of the extracellular matrix, leads to an increased pro-inflammatory response. In some studies, low-volume injury was shown to predominate [13, 14, 17], whereas in others, including laboratory [18] and clinical studies [19], overdistension was the prevailing VILI mechanism.

## Lung Inflammation Assessed by Positron Emission Tomography

Since inflammation in the lung seems to be a mediator in all causes of VILI [15, 20] and neutrophils play an important role in the inflammatory response to injurious mechanical ventilation [21], a research tool suitable for tracking regional inflammatory responses in the course of VILI and during lung protective ventilation strategies is of great interest.

Positron emission tomography (PET) is an advanced nuclear medicine technique used for non-invasive and quantitative measurements of radioactivity concentration within living tissues. It is based on the physical properties of certain isotopes that, when decaying, emit a positron, a particle with a mass equal to an electron but with a positive charge. The positron almost immediately collides with an electron and both are annihilated. In this process, two high-energy photons are created and leave the site of annihilation in opposite directions. The PET scanner is equipped with a large number of scintillation detectors arranged in a ring surrounding the object of interest. When two photons with equal energies are detected in coincidence, the event is stored in a dedicated data array called a sinogram. Typically,

many millions of coincidences are stored during a PET scan. Coincidences are collected for a finite amount of time, called a time-frame. With modern PET scanners, a time-frame can range from a few seconds up to several minutes. Dynamic PET is a term used when several time-frames are collected from the same area of the body to track the changes in radioactivity concentration over time. The complete sinogram is then converted into a three-dimensional data array in a process called image reconstruction. Each data entry in this new data array contains the actual radioactivity concentration of a certain portion of the body within the specified time-frame. The three-dimensional image array can be viewed as a stack of tomographic slices on a computer display with color codes for the actual radioactivity concentration. When kinetic information is wanted, the dynamic PET data are processed further with dedicated computer software. Regions of interest are placed at will within the tissue and data resembling the changes in concentration over time are extracted. In advanced kinetic analysis, the time-activity curves of both the blood and the tissue of interest are needed. Advanced kinetic analysis typically involves the use of computer-aided mathematical modeling.

In ALI, the non-barrier functions of the pulmonary endothelium have been emphasized. But the barrier function *per se* is essential in preserving the most important purpose of the lungs: the adequate exchange of respiratory gases. PET studies have shown that measures of barrier function are a non-specific index of lung injury, indicating functional not structural lung injury [22, 23]. For example, PET imaging methods allow the rate at which proteins move across the endothelial barrier from vascular to extravascular compartments to be measured, the so called pulmonary transcapillary escape rate (PTCER). Palazzo et al. [24] used PET imaging to measure PTCER in an *in vivo* canine model of unilateral pulmonary ischemia-reperfusion injury and found that it was increased in the ischemic lung. Interestingly, both lungs had an increased PTCER compared with control non-ischemic lungs, suggesting that injury in one lung can lead to similar injury in the contralateral lung, a finding that has been observed in an analogous clinical setting, such as acute unilateral pneumonia. Calandrino et al. [22] described that, while PTCER and extravascular density, a close correlate to extravascular lung water (EVLW), were both elevated in ARDS patients they correlated poorly with one another on a regional basis. Moreover, as extravascular density returned to normal, PTCER remained elevated suggesting that lung tissue injury might be 'subclinical' but still present, even after pulmonary edema has actually resolved. This observation was further confirmed by Sandiford et al. [25] who examined the regional distribution of PTCER and extravascular density more closely in ARDS patients and found ventral-dorsal gradients only for extravascular density but not for PTCER. Once more, functional injury was detected even in lung regions that appeared to be free of structural injury. The finding that the lungs of ARDS patients are more diffusely involved than what might otherwise be assumed from just structural radiological imaging, such as computed tomography (CT), helps explain why ARDS lungs are so vulnerable to VILI: radiographically 'normal' lung, i. e., lung with a normal EVLW content in non-dependent lung regions may still be abnormal and vulnerable to mechanical stresses caused by mechanical venti-

lation. These data tell us that non-dependent regions of ARDS lung are 'at risk' because they demonstrate subclinical evidence of injury, which can be made manifest by inappropriate ventilator use. Jones et al. [26] showed a surprisingly high pulmonary uptake of [$^{18}$F]-fluorodeoxyglucose ($^{18}$F-FDG) in patients with head injury at risk of developing ARDS but without lung symptoms at the time of the scan. This signal may reflect sequestration of primed neutrophils in lung capillaries. *In vitro* studies in isolated human neutrophils have demonstrated that the uptake of deoxyglucose is increased to the same extent in cells that are only primed or primed and stimulated [27]. This finding indicates the vulnerability of these patients while on ventilatory support, because, even though neutrophils remain in a primed state, any additional stimulus precipitates actual tissue damage.

PET with $^{18}$F-FDG, a glucose-analog tracer, offers the opportunity to study regional lung inflammation *in vivo* with the advantage over conventional histological methods of preserving the integrity of the lung. $^{18}$F-FDG is taken up predominantly by metabolically active cells and has been recognized as a key marker of neutrophilic inflammation in the inflamed non-tumoral lung [14, 21, 28–33].

The type of lung cells responsible for $^{18}$F-FDG uptake ($K_i$) has been the matter of extensive investigation in models of ALI. $^{18}$F-FDG is a non-specific tracer, because it labels any cell with intense glucose uptake. However, several studies performed in humans [34] and animal models [29] have shown that, during pulmonary inflammation, most of the $^{18}$F-FDG uptake as measured by $K_i$ can be attributed to activated neutrophils [35], even when macrophages are more abundant [30]. Although not usually characterized by an intense $^{18}$F-FDG uptake [36], macrophages may play a role in the generation of VILI [37]. The latest evidence [38] suggests that macrophages, as well as type 2 epithelial cells, might contribute to the $^{18}$F-FDG uptake signal during VILI. Therefore, although the overall $^{18}$F-FDG uptake signal is a complex mixture of the metabolic activity of many cell types, prior [29, 34–36] and very recent studies [17] have established that the major influence on the regional signal is the high metabolic activity of recruited neutrophils. In the acutely injured lung, images can therefore be interpreted, with a good approximation, as the regional distribution of neutrophilic inflammation.

There is a theoretical concern that in ALI, $^{18}$F-FDG may leak to the alveolar spaces becoming a major and non-specific determinant of the $^{18}$F-FDG signal, potentially causing a false, non-inflammation related increase in the measured uptake ($K_i$). The presence of edema, however, does not seem to affect the measurement of $K_i$, as suggested by Chen and Schuster [29], who measured glucose uptake with $^{18}$F-FDG in anesthetized dogs after intravenous oleic acid-induced ALI or after low-dose intravenous endotoxin followed by oleic acid. The rate of $^{18}$F-FDG uptake was significantly elevated in both endotoxin-treated groups, but not in the group treated only with oleic acid, leading the authors to conclude that pulmonary vascular leak, and consequently edema, does not significantly contribute to the $K_i$ in ARDS lungs.

## Higher Uptake in Normally and Poorly Aerated Lung

This *in vivo* non-invasive molecular imaging method has brought new insights into the role of low-volume vs. high-volume injury mechanisms [14, 32, 39]. Increased inflammation was found in normally aerated lung regions in a mixed population of patients with ARDS [39], an interesting finding differing from the classically assumed VILI targets in either overstretched or collapsed lung regions. Although thought-provoking, the study could not locate the regional onset of lung inflammation or determine the relative importance of the different mechanisms of VILI, as studied patients ranged in severity and duration of their ARDS.

We proceeded one step further by studying the location and magnitude of early inflammatory changes using PET imaging of $^{18}$F-FDG in a porcine experimental model of ARDS. We evaluated the individual contributions of regional injurious mechanisms during early stages of VILI. To accomplish this aim, we created an experimental VILI model and designed a study that produced lungs heterogeneously aerated with significant amounts of non-aerated, poorly and normally aerated, and hyperinflated lung tissue (shown by CT). Within the same lung, we simultaneously found tidal hyperinflation, predominantly located in the non-dependent lung region, and collapse with tidal recruitment, mostly located in the dependent region. Remarkably, these two regions, classically comprising the major mechanisms of VILI, had $^{18}$F-FDG uptakes similar to the healthy control group. On the other hand, the remaining regions situated in the intermediate portions of the lung presented a significantly higher uptake. Similarly, in the normal and poorly aerated regions we found the highest differences in $^{18}$F-FDG uptake as compared to healthy controls, whereas the hyperinflated and non-aerated regions were similar to the control group (Fig. 1). We believe these findings challenge the current notion that hyperinflation and/or repeated collapse and re-expansion of alveolar units play the major role in early VILI. Instead, our data suggest that tidal stretch was highest in the poorly and normally aerated regions and this mechanism is the most important trigger of inflammation in these conditions. They also support the concept that the smaller the ventilated lung, the higher the VILI-triggering forces will be, as a larger fraction of $V_T$ is delivered to a smaller lung volume.

An intriguing yet unanswered question raised by our data is whether the increased susceptibility to VILI was related to small length-scale heterogeneities of the lung parenchyma or of the airways [40], below the resolution limit of the CT, occurring in the poorly or even in the normally aerated regions. These heterogeneities would tend to produce an uneven distribution of $V_T$ within lung regions and might have contributed to VILI. Perlman and Bhattacharya used real-time confocal microscopy to determine the micromechanics of alveolar perimeter distension in perfused rat lungs [41]. These investigators were able to image a 2-μm thick optical section under the pleura. Five to eight segments were identified within each alveolus. The average length of these segments was compared during normal inflation and hyperinflation. They found segmental distension to be heterogeneous within a single alveolus. Similarly, by using synchrotron-based X-ray tomographic

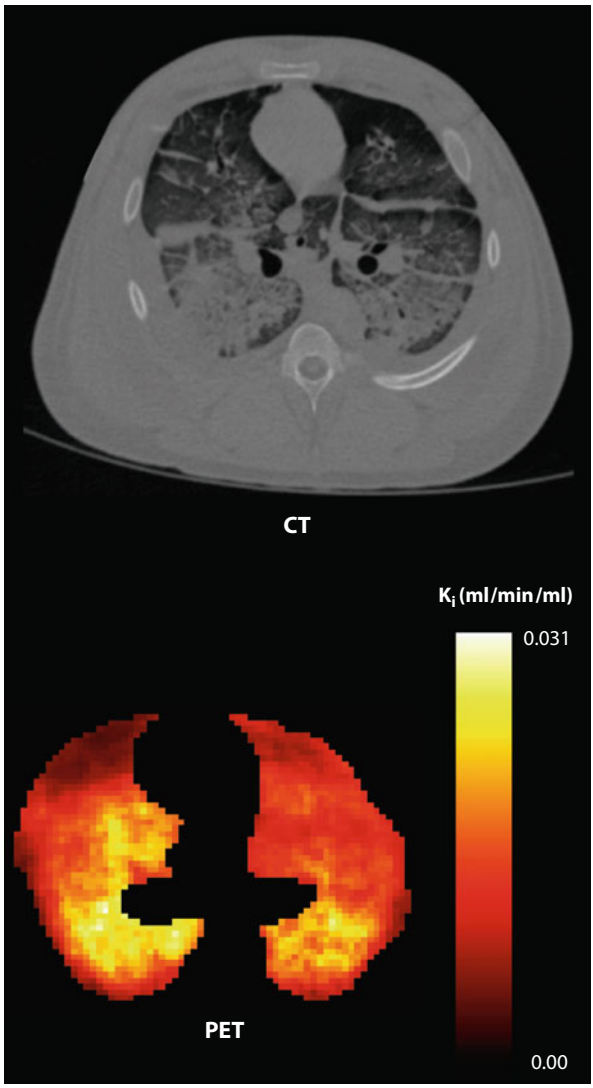


**Fig. 1** Representative positron emission tomography (PET) image of net [$^{18}$F]fluoro-2-deoxy-D-glucose ($^{18}$F-FDG) uptake rate ($K_i$) in an experimental model of ventilator-induced lung injury. Note the predominance of activity in the normal and poorly aerated regions as seen in the corresponding computed tomography (CT) image

microscopy on isolated rat lungs, Rausch et al. [42] estimated that local strains developing in alveolar walls were as much as four times higher than the global, with 'strain hotspots' occurring within the thinnest parts of the alveolar walls. When studying 3D microscopic distribution of lung parenchyma, using it as an input to their finite element modeling of alveolar expansion, they observed that thin regions may become overstretched, whereas regions with tissue accumulation remain unchallenged. These data fit with our own results and strongly suggest that a tidal stretch of the 'healthy' aerated parts of the heterogeneous aerated ARDS lungs can play a primary role in the activation of the inflammatory signaling cascade.

Furthermore, our finding of increased inflammation in normally aerated regions is in agreement with those of Bellani and colleagues [39] who, in their study of ARDS patients, determined that the metabolic activity of aerated regions was associated with both plateau pressure and regional $V_T$ normalized by end-expiratory lung gas. Interestingly, neither they nor we found an association between cyclic alveolar recruitment-derecruitment and increased metabolic activity. Some key differences between this clinical study and our experimental observations highlight their complementary nature in terms of understanding VILI: 1) the time on mechanical ventilation before the clinical PET study averaged nine days and ranged from two to sixteen days, likely mixing distinct phases of ARDS and VILI pathophysiology, whereas our experimental study focused on early (hours) ARDS; 2) patients had limited tidal recruitment (2.9 % of the total lung weight) due to the lung-protective mechanical ventilation strategy applied, raising the question whether conditions with higher tidal recruitment would have produced more inflammation in those or in other regions, which our experimental data ruled out; 3) likewise, the amount of tissue undergoing hyperinflation was much smaller in the clinical study compared to our experimental study, because of the relatively low plateau pressures and $V_T$ used in the patients. We observed that, even in more extreme ventilatory conditions with significant amounts of collapse, tidal recruitment, and hyperinflation, lung inflammation still predominates in the poorly and normally aerated regions.

At least three mechanisms could explain the increased $K_i$ in poorly aerated regions: 1) alveolar cyclic recruitment at the subvoxel level; 2) cyclic opening and closing of small airways; or 3) increased tidal stretch. Measurements based on fluorescent microspheres confirmed the existence of ventilation heterogeneity down to length scales of 2 $cm^3$ [43], and findings from synchrotron CT suggested that heterogeneity of specific ventilation (defined as ventilation per unit gas volume) can occur at lung volumes as low as 1 $mm^3$ [44]. Recently, Wellman et al. have elegantly developed methods using PET to assess heterogeneity of specific ventilation at length scales below and above the effective image resolution of 12 mm [40]. Sub-resolution specific ventilation heterogeneity was reflected by multi-compartment voxel-level tracer kinetics during washout of [$^{13}$N]nitrogen ($^{13}$NN) from alveolar air space. These authors modeled the washout kinetics of $^{13}$NN with PET to examine how specific ventilation heterogeneity at different length scales was influenced by lung aeration. They showed that airway narrowing or alveolar derecruitment can occur in poorly aerated lung regions especially at low length scales with a significant component derived from sub-resolution (< 12 mm) length scales. Components of specific ventilation heterogeneity at all studied length scales (< 12 to 60 mm) were highest in poorly aerated regions. Rylander et al., when studying the size and distribution of a "poorly aerated" compartment in ARDS patients, observed an uneven distribution of ventilation due to the presence of small-airway closure and/or obstruction [45]. Of note, airway dysfunction has been increasingly recognized as an important contributor to pulmonary impairment in patients with ARDS [46]. Animal models of ARDS have shown that, in addition to damage to the parenchyma, small airway injuries are characterized by bronchiolar epithelial

necrosis and sloughing and by rupture of alveolar-bronchiolar attachments [47]. In humans who died with ARDS, small airway changes were characterized by wall thickening with inflammation, extracellular matrix remodeling, and epithelial denudation [46, 48].

Putting together all these aspects, it seems that, during VILI, the collapsed dependent and hyperinflated non-dependent regions may indirectly damage the normally and poorly aerated lung regions, by diverting the $V_T$ to those regions submitting them to higher tidal stretch. We believe that the local consequences of the stretch in non-dependent regions and the local consequences of the mechanisms related to collapse in dependent regions are less important than the remote consequent stretches inflicted to the remainder intermediately located "baby lung" in terms of regional inflammation. Our findings highlight that we cannot determine which mechanism of VILI is more critical to oppose, but rather they emphasize the importance of strategies capable of minimizing both, collapse and hyperinflation, thereby unloading the small-aerated lung.

The effects of a protective ventilation strategy on topographic lung inflammatory cell activity have been recently described [17]: In a model of endotoxemic ALI, de Prost et al. found that mechanical ventilation had an important effect in determining the regional distribution and degree of early neutrophilic inflammation. When comparing protective ventilation ($V_T$ 8 mL/kg and PEEP titrated to obtain a plateau pressure (Pplat) of 30 $cmH_2O$) with injurious ventilation (zero PEEP and $V_T$ titrated to obtain a Pplat of 30 $cmH_2O$), the former resulted in a more homogeneously distributed uptake. Their findings are compatible with the concept that ventilation strategy plays an early pathogenic role in determining the profile of inflammatory cell distribution before lung injury is established and emphasize that the prevention of VILI should be a key aspect of patient management, even when mechanical ventilation periods and the underlying level of injury are limited [49]. Such results support former suggestion that heterogeneous inflammation may be an important element in the pathogenesis of ARDS [13]. Of note, these results indicate that in early endotoxemia during mechanical ventilation with no PEEP, inflammation predominates in the dependent regions.

## Perspectives

As we have discussed, PET provides unique and unprecedented information to shed light on the inflammatory component of ARDS and VILI. The development of new and more selective/specific tracers to detect early inflammation has the potential to further enhance PET's capabilities and contributions. TNF-$\alpha$ is a well-known pro-inflammatory cytokine produced by monocytes and macrophages. It mediates the immune response by recruiting white blood cells to sites of inflammation and is involved in acute responses to injury. TNF-$\alpha$ appears in the circulation during the onset of sepsis-induced lung injury and is suggested to be an important early mediator of ALI. Interestingly, neutrophil recruitment induced by pure mechanical lung stretch has a significant TNF-$\alpha$ component [50].

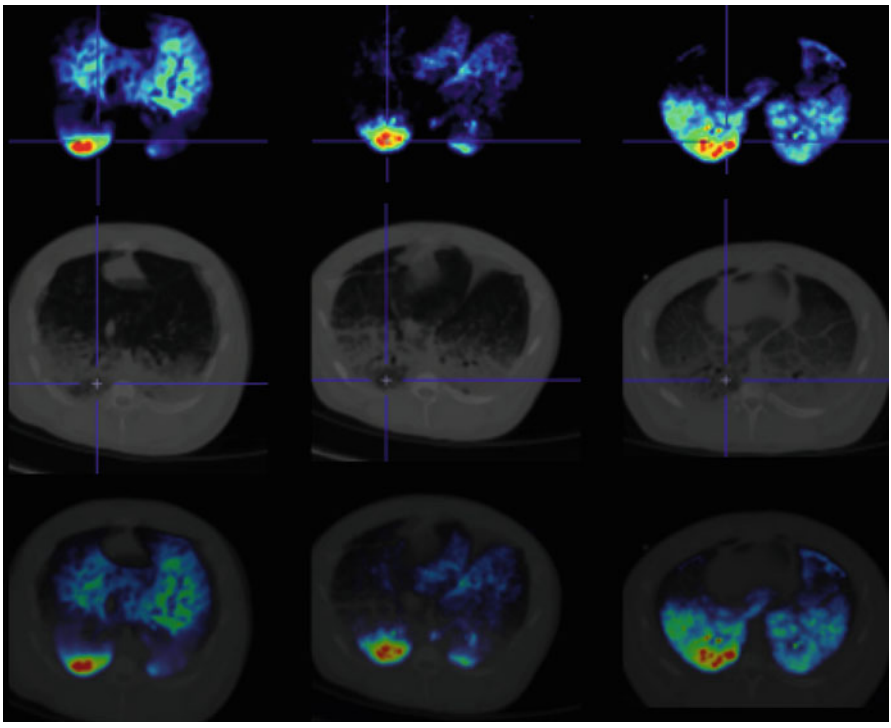

**Fig. 2** Animals submitted to an experimental model of VILI were studied with positron emission tomography/computed tomography (PET/CT). PET images of the lung were obtained dynamically after injection of a tracer based on TNF-$\alpha$. The images were generated with a novel approach with the pre-normalization of data before application of principal component analysis (PCA). PCA is a multivariate technique that has become an attractive tool in analyzing dynamic PET images because is a data-driven technique that emphasizes the regions with different kinetics without modeling assumptions. Three different slices at three different levels from the same animal are shown. Coloring is according to a relative scale for each image with black representing minimal and red maximal activity. Note the predominance of the activity in the poorly aerated regions

We have explored a new meaningful PET tracer based on TNF-$\alpha$ using a fusion protein of two affibody molecules fused genetically. Affibody molecules are a class of small protein domains that compete with receptor binding and have been shown to function as good imaging agents in the clinical setting. In preliminary tests *in vivo*, using an experimental model of ARDS, we tested a novel positron-emitting ligand of gallium, $^{68}$Ga-TNF$\alpha$. In the same way as with $^{18}$F-FDG, PET images were obtained dynamically and at the end of the experiment tissue samples were taken from the lung and the abdomen. Significant activity inside the lung tissue was evidenced on the PET/CT images (Fig. 2). Tissue samples showed TNF-$\alpha$ (as analyzed with enzyme-linked immunosorbent assay [ELISA]) in the lung parenchyma and in small intestine tissue 4 hours after establishing the lung injury model. We confirmed that the used ligand of TNF-$\alpha$ bound to inflamed lung tissue and thus

may become a future useful marker of inflammation especially when repeated studies are desirable.

## Conclusions

Dynamic PET/CT imaging of $^{18}$F-FDG has provided new relevant information on the location and distribution of inflammation in early VILI. The findings suggest that normally and poorly aerated regions – corresponding to intermediate gravitational zones – are the primary targets of the inflammatory process accompanying early VILI. This may be attributed to the small aerated lung volume that receives most of the ventilation and has potential implications in the way we approach lung protective ventilation.

## References

1. Celsus AC (1478) Cornelii Celsi De medicina liber incipit. A Nicolao [Laurentii] impressvs, Florentiae
2. Rather LJ (1971) Disturbance of function (functio laesa): the legendary fifth cardinal sign of inflammation, added by Galen to the four cardinal signs of Celsus. Bull N Y Acad Med 47:303–322
3. Mueller K (2013) Inflammation. Inflammation's yin-yang. Introduction. Science 339:155
4. Phua J, Badia JR, Adhikari NKJ et al (2009) Has mortality from acute respiratory distress syndrome decreased over time?: A systematic review. Am J Respir Crit Care Med 179:220–227
5. Malhotra A, Drazen JM (2013) High-Frequency Oscillatory Ventilation on Shaky Ground. N Engl J Med 368:863–865
6. Rubenfeld GD, Caldwell E, Peabody E et al (2005) Incidence and outcomes of acute lung injury. N Engl J Med 353:1685–1693
7. Ware LB, Matthay MA (2000) The acute respiratory distress syndrome. N Engl J Med 342:1334–1349
8. Matthay MA, Zimmerman GA (2005) Acute lung injury and the acute respiratory distress syndrome: four decades of inquiry into pathogenesis and rational management. Am J Respir Cell Mol Biol 33:319–327
9. Matthay MA, Ware LB, Zimmerman GA (2012) The acute respiratory distress syndrome. J Clin Invest 122:2731–2740
10. Santos Dos CC, Slutsky AS (2000) Invited review: mechanisms of ventilator-induced lung injury: a perspective. J Appl Physiol 89:1645–1655
11. Vlahakis NE, Hubmayr RD (2005) Cellular stress failure in ventilator-injured lungs. Am J Respir Crit Care Med 171:1328–1342
12. Malhotra A (2007) Low-tidal-volume ventilation in the acute respiratory distress syndrome. N Engl J Med 357:1113–1120
13. Otto CM, Markstaller K, Kajikawa O et al (2008) Spatial and temporal heterogeneity of ventilator-associated lung injury after surfactant depletion. J Appl Physiol 104:1485–1494
14. de Prost N, Costa EL, Wellman T et al (2011) Effects of surfactant depletion on regional pulmonary metabolic activity during mechanical ventilation. J Appl Physiol 111:1249–1258
15. Tremblay L, Valenza F, Ribeiro SP et al (1997) Injurious ventilatory strategies increase cytokines and c-fos m-RNA expression in an isolated rat lung model. J Clin Invest 99:944–952

16. Dreyfuss D, Saumon G (1998) Ventilator-induced lung injury: lessons from experimental studies. Am J Respir Crit Care Med 157:294–323
17. de Prost N, Costa EL, Wellman T et al (2013) Effects of ventilation strategy on distribution of lung inflammatory cell activity. Crit Care 17:R175
18. Tsuchida S, Engelberts D, Peltekova V et al (2006) Atelectasis causes alveolar injury in nonatelectatic lung regions. Am J Respir Crit Care Med 174:279–289
19. Terragni PP, Rosboch G, Tealdi A et al (2007) Tidal hyperinflation during low tidal volume ventilation in acute respiratory distress syndrome. Am J Respir Crit Care Med 175:160–166
20. Ranieri VM, Suter PM, Tortorella C et al (1999) Effect of mechanical ventilation on inflammatory mediators in patients with acute respiratory distress syndrome: a randomized controlled trial. JAMA 282:54–61
21. Musch G, Venegas JG, Bellani G et al (2007) Regional gas exchange and cellular metabolic activity in ventilator-induced lung injury. Anesthesiology 106:723–735
22. Calandrino FSJ, Anderson DJ, Mintun MA, Schuster DP (1988) Pulmonary vascular permeability during the adult respiratory distress syndrome: a positron emission tomographic study. Am Rev Respir Dis 138:421–428
23. Schuster DP (1995) What is acute lung injury? What is ARDS? Chest 107:1721–1726
24. Palazzo R, Hamvas A, Shuman T et al (1992) Injury in nonischemic lung after unilateral pulmonary ischemia with reperfusion. J Appl Physiol 72:612–620
25. Sandiford P, Province MA, Schuster DP (1995) Distribution of regional density and vascular permeability in the adult respiratory distress syndrome. Am J Respir Crit Care Med 151:737–742
26. Jones HA, Clark JC, Minhas PS et al (1998) Pulmonary neutrophil activation following head trauma. Am J Respir Crit Care Med 157:A349 (abst)
27. Jones HA, Cadwallader KA, White JF et al (2002) Dissociation between respiratory burst activity and deoxyglucose uptake in human neutrophil granulocytes: implications for interpretation of (18)F-FDG PET images. J Nucl Med 43:652–657
28. Bellani G, Messa C, Guerra L et al (2009) Lungs of patients with acute respiratory distress syndrome show diffuse inflammation in normally aerated regions: a [$^{18}$F]-fluoro-2-deoxy-D-glucose PET/CT study. Crit Care Med 37:2216–2222
29. Chen DL, Schuster DP (2004) Positron emission tomography with [$^{18}$F]fluorodeoxyglucose to evaluate neutrophil kinetics during acute lung injury. Am J Physiol Lung Cell Mol Physiol 286:L834–L840
30. Jones HA, Clark RJ, Rhodes CG et al (1994) In vivo measurement of neutrophil activity in experimental lung inflammation. Am J Respir Crit Care Med 149:1635–1639
31. Jones HA, Sriskandan S, Peters AM et al (1997) Dissociation of neutrophil emigration and metabolic activity in lobar pneumonia and bronchiectasis. Eur Respir J 10:795–803
32. Costa ELV, Musch G, Winkler T et al (2010) Mild endotoxemia during mechanical ventilation produces spatially heterogeneous pulmonary neutrophilic inflammation in sheep. Anesthesiology 112:658–669
33. de Prost N, Tucci MR, Melo MFV (2010) Assessment of lung inflammation with $^{18}$F-FDG PET during acute lung injury. AJR Am J Roentgenol 195:292–300
34. Chen DL, Rosenbluth DB, Mintun MA, Schuster DP (2006) FDG-PET imaging of pulmonary inflammation in healthy volunteers after airway instillation of endotoxin. J Appl Physiol 100:1602–1609
35. Oehler R, Weingartmann G, Manhart N et al (2000) Polytrauma induces increased expression of pyruvate kinase in neutrophils. Blood 95:1086–1092
36. Jones HA, Schofield JB, Krausz T et al (1998) Pulmonary fibrosis correlates with duration of tissue neutrophil activation. Am J Respir Crit Care Med 158:620–628
37. Wilson MR, O'Dea KP, Zhang D et al (2009) Role of lung-marginated monocytes in an in vivo mouse model of ventilator-induced lung injury. Am J Respir Crit Care Med 179:914–922

38. Saha D, Takahashi K, de Prost N et al (2013) Micro-autoradiographic assessment of cell types contributing to 2-deoxy-2-[(18)F]fluoro-D-glucose uptake during ventilator-induced and endotoxemic lung injury. Mol Imaging Biol 15:19–27
39. Bellani G, Guerra L, Musch G et al (2011) Lung regional metabolic activity and gas volume changes induced by tidal ventilation in patients with acute lung injury. Am J Respir Crit Care Med 183:1193–1199
40. Wellman TJ, Winkler T, Costa ELV et al (2012) Effect of regional lung inflation on ventilation heterogeneity at different length scales during mechanical ventilation of normal sheep lungs. J Appl Physiol 113:947–957
41. Perlman CE, Bhattacharya J (2007) Alveolar expansion imaged by optical sectioning microscopy. J Appl Physiol 103:1037–1044
42. Rausch SMK, Haberthur D, Stampanoni M et al (2011) Local Strain Distribution in Real Three-Dimensional Alveolar Geometries. Ann Biomed Eng 39:2835–2843
43. Robertson HT, Altemeier WA, Glenny RW (2000) Physiological implications of the fractal distribution of ventilation and perfusion in the lung. Ann Biomed Eng 28:1028–1031
44. Porra L, Monfraix S, Berruyer G et al (2004) Effect of tidal volume on distribution of ventilation assessed by synchrotron radiation CT in rabbit. J Appl Physiol 96:1899–1908
45. Rylander C, Tylén U, Rossi-Norrlund R et al (2005) Uneven distribution of ventilation in acute respiratory distress syndrome. Crit Care 9:R165–R171
46. Pires-Neto RC, Morales MMB, Lancas T et al (2013) Expression of acute-phase cytokines, surfactant proteins, and epithelial apoptosis in small airways of human acute respiratory distress syndrome. J Crit Care 28:111.e9–111.e15
47. D'Angelo E, Koutsoukou A, Della Valle P et al (2008) Cytokine release, small airway injury, and parenchymal damage during mechanical ventilation in normal open-chest rats. J Appl Physiol 104:41–49
48. Morales MMB, Pires-Neto RC, Inforsato N et al (2011) Small airway remodeling in acute respiratory distress syndrome: a study in autopsy lung tissue. Crit Care 15:R4
49. Fernandez-Perez ER, Keegan MT, Brown DR et al (2006) Intraoperative tidal volume as a risk factor for respiratory failure after pneumonectomy. Anesthesiology 105:14–18
50. Wilson MR, Choudhury S, Takata M (2005) Pulmonary inflammation induced by high-stretch ventilation is mediated by tumor necrosis factor signaling in mice. Am J Physiol Lung Cell Mol Physiol 288:L599–L607